Journal of The Electrochemical Society, **151** (2) G93-G97 (2004)
0013-4651/2004/151(2)/G93/5/$7.00 © The Electrochemical Society, Inc.

Leakage and Breakdown Mechanisms of Cu Comb Capacitors with Bilayer-Structured α-SiCN/α-SiC Cu-Cap Barriers

Chiu-Chih Chiang,[a,z] I-Hsiu Ko,[a] Mao-Chieh Chen,[a,*] Zhen-Cheng Wu,[b] Yung-Cheng Lu,[b] Syun-Ming Jang,[b] and Mong-Song Liang[b]

[a]*Department of Electronics Engineering, National Chiao-Tung University, Hsinchu 300, Taiwan*
[b]*Department of Dielectric and CMP, Advanced Module Technology Division, Taiwan Semiconductor Manufacturing Company, Science-Based Industrial Park, Hsinchu, Taiwan*

This work investigates the leakage and breakdown mechanisms in copper (Cu) comb capacitors with carbon-doped low-*k* plasma-enhanced chemical vapor deposited organosilicate glass (OSG; $k = 3$) as the intermetal dielectric and an α-SiCN ($k = 5$)/α-SiC ($k = 4$) bilayer-structured dielectric film as the Cu-cap barrier. The leakage mechanism between Cu lines is dependent on the thickness ratio of the α-SiCN/α-SiC bilayer barrier. Using an α-SiCN/α-SiC bilayer barrier of 40 nm/10 nm or 30 nm/20 nm bilayer thickness, the increased leakage current (Frenkel-Poole emission) between Cu lines is attributed to the large number of interfacial defects, such as cracks, voids, traps or dangling bonds at the α-SiC/OSG interface, which are generated by the larger tensile force of the thicker α-SiC film. The Cu comb capacitor with an α-SiCN (50 nm)/α-SiC (2 nm) bilayer barrier exhibits a much smaller leakage current. The breakdown field and time-dependent dielectric breakdown lifetime of the Cu comb capacitor reveal little dependence on the thickness ratio of the α-SiCN/α-SiC bilayer barrier, and the observed breakdown of the Cu comb capacitor is presumably due to dielectric breakdown of the bulk OSG layer.
 [DOI: 10.1149/1.1639169]

Manuscript submitted April 23, 2003; revised manuscript received August 29, 2003. Available electronically January 8, 2004.

As the interconnect resistance-capacitance (RC) delay becomes a dominant factor in determining the performance of integrated circuits, the advantages of Cu metal and low-*k* dielectrics become more remarkable. Cu metal reduces the electrical resistance of interconnection lines because of its low electrical resistivity; moreover, Cu line also exhibits a better electromigration resistance than the conventional Al-based wires. The use of low-*k* dielectrics in the interconnect system reduces the wire capacitance, signal-propagation delay, cross talk-noise between metal lines, and power dissipation of integrated circuits. While many low-*k* ($k < 3$) materials have been used as inter- and intralayer dielectrics (ILD), high-dielectric-constant ($k > 7$) silicon nitride is still the primary candidate for the Cu-cap barrier and etching stop layer (ESL) required in the Cu damascene structure. It is desirable to replace silicon nitride with dielectric materials of lower *k*-value ($k < 5$) in order to further reduce the effective dielectric constant of the Cu interconnect system. In recent years, amorphous silicon carbides (α-SiC) and amorphous silicon-nitricarbide (α-SiCN) deposited by plasma-enhanced chemical vapor deposition (PECVD) using organosilicate gases (OSG) are receiving extensive attention for applications as Cu-cap barriers and ESL in Cu interconnection schemes because of their lower *k*-value, better etching selectivity with OSG, robust chemical mechanical polishing (CMP) strength, good photoresist poisoning resistance, higher antireflective ability, and superior properties as a Cu barrier/passivation layer in terms of Cu restraint, electromigration resistance, and Cu-hillock density.[1-3] There are a number of studies on the electrical reliability of the α-SiC and α-SiCN films with respect to their integration with Cu using planar metal-insulator-semiconductor (MIS) capacitors.[3-6] In practical applications, however, considerable attention must be focused on the electrical reliability issues of comb capacitors, such as leakage and breakdown mechanisms and potential leakage paths in the bulk of the low-*k* film, the Cu-cap barrier/low-*k* film interface, and the surrounding dielectrics. It was found in our previous work that the bilayer-structured α-SiCN/α-SiC dielectric film is a favorable combination to serve as a Cu-cap barrier to improve time-dependent dielectric breakdown (TDDB) reliability of the Cu comb capacitor.[6] The improvement in TDDB is due to the α-SiC film's lower leakage current, better adhesion to Cu and OSG IMD, and absence of nitridation on the Cu surface. The α-SiCN film on top of the α-SiC film serves to protect the α-SiC film from plasma attack, such as O_2 plasma attack during photoresist stripping and organosilicate plasma attack during OSG deposition. In this work, we investigate the leakage and breakdown mechanisms in the Cu comb capacitor with a bilayer-structured α-SiCN/α-SiC Cu-cap barrier.

Experimental

The leakage current of Cu comb capacitors was measured on a 0.12/0.12 μm (linewidth/space) comb capacitor as illustrated in Fig. 1. A 40 nm PECVD amorphous silicon-oxycarbide (α-SiCO) ESL was deposited on the PECVD oxide ILD. A single-level Cu damascene (Metal-1) process with a 250 nm PECVD methylsilane-based low-*k* OSG ($k = 3$) as the IMD was employed to fabricate the comb capacitor. After patterning of 0.12/0.12 μm linewidth/space trenches in the OSG/ESL/ILD dielectric stack, the damascene Cu feature was electrochemically deposited on a 15 nm physical vapor deposited (PVD) TaN liner barrier. Following the Cu CMP, a bilayer-structured α-SiCN ($k = 5$)/α-SiC ($k = 4$) Cu-cap barrier with a bilayer thickness of 50/2, 45/5, 40/10, and 30/20 (nm/nm) was sequentially deposited in a PECVD system at 350°C and a total gas pressure of 1-5 Torr. The α-SiC film was deposited using $(CH_3)_3SiH$ with a flow rate of 100-500 sccm and a plasma power of 100-200 W, while the α-SiCN layer was deposited using

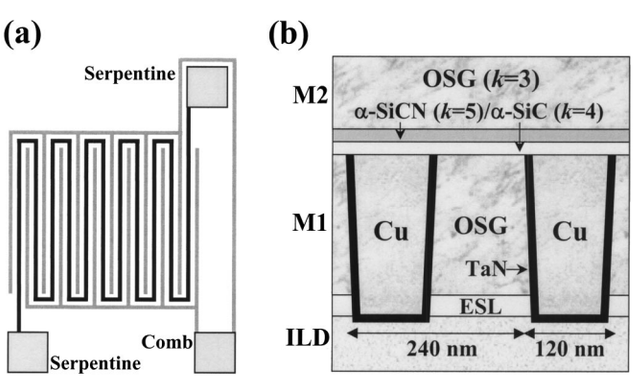

Figure 1. Schematic (a) top-view and (b) cross-sectional view of the Cu comb capacitor test structure employed in this study.

* Electrochemical Society Active Member.
z E-mail: cchiang.ee88g@nctu.edu.tw

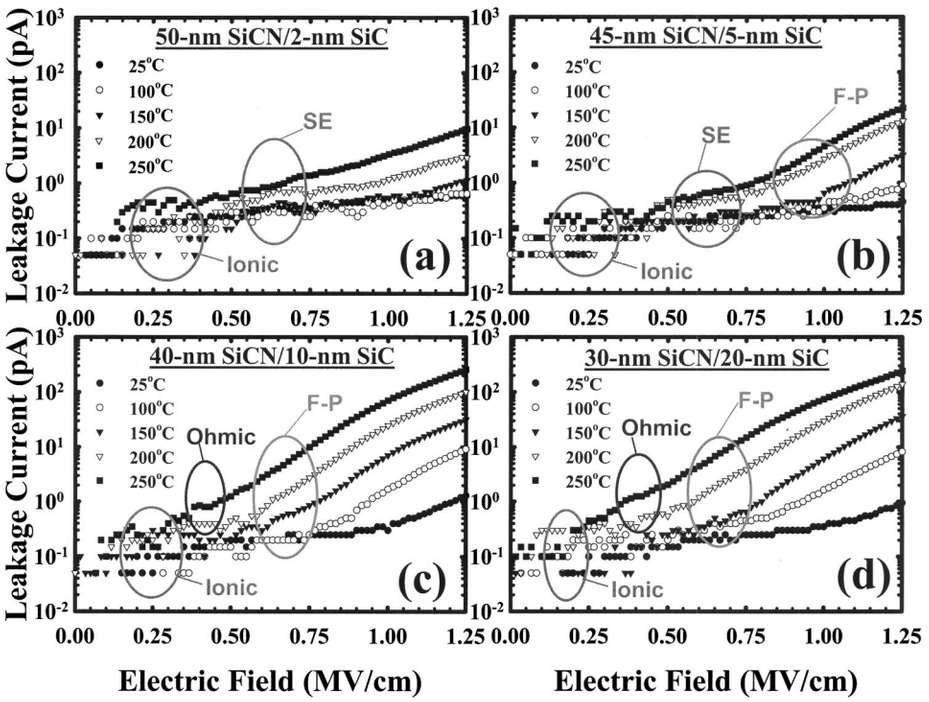

Figure 2. Leakage current *vs.* electric field, measured at various temperatures, for Cu comb capacitor using a bilayer-structured Cu-cap barrier with an α-SiCN/α-SiC bilayer thickness of (a) 50/2, (b) 45/5, (c) 40/10, and (d) 30/20 (nm/nm).

$He/(CH_3)_3SiH/NH_3$ with a flow ratio of 8/3/6 and a plasma power of 100-500 W. Another layer of PECVD OSG was deposited for the next Cu damascene (Metal-2) process.

An HP4145B semiconductor parameter analyzer was used to measure the leakage current between Cu lines and provide the bias for the bias-temperature-stress (BTS) test. An N_2 purging was used to prevent possible oxidation of the Cu metal and moisture uptake in the dielectric films during the measurement. Raphael modeling[c] was used to obtain the distribution of electric field in the Cu comb capacitors.

Results and Discussion

Figure 2 shows the leakage current of Cu comb capacitors with an α-SiCN/α-SiC bilayer barrier of different thickness ratios measured at various temperatures. The dominant current conduction mechanisms in the Cu comb capacitors were identified by fitting slopes for various conduction mechanisms, as shown in Fig. 3. Evidently, the fitting slopes vary with the electric field. All comb capacitors exhibit ionic conduction at electric fields below 0.5 MV/cm for all measurement temperatures. The ionic current shows a hysteresis effect (Fig. 3a), as confirmed by repeatedly sweeping the electric field from −1.25 to +1.25 MV/cm and back down.[7,8] The ionic conduction of Cu comb capacitors becomes more apparent at low temperatures (*e.g.*, 25°C), whereas a conduction mechanism like ohmic conduction prevails at temperatures above 200°C. Notably, the comb capacitors with an α-SiCN/α-SiC bilayer barrier of 40 nm/10 nm or 30 nm/20 nm thickness exhibit ohmic conduction at electric fields between 0.25 and 0.5 MV/cm and at temperatures of 200-250°C; in this region, the leakage current (I) is linearly correlated with the electric field (E) (Fig. 3b), and the current can be expressed by Eq. 1.[7] The comb capacitor with an α-SiCN/α-SiC bilayer barrier of 50 nm/2 nm thickness exhibits Schottky emission (SE) at electric fields above 0.5 MV/cm, particularly at temperatures above 200°C. The SE conduction shows $\ln(I/T^2)$ linearly correlated with $E^{1/2}$ (Fig. 3c), and the current can be expressed by Eq. 2.[7] Nevertheless, the comb capacitor with an α-SiCN/α-SiC bilayer barrier of 45 nm/5 nm thickness exhibits SE conduction only at electric fields of 0.5-0.8 MV/cm, and Frenkel-Poole (F-P) emission appears after the kink at 0.8 MV/cm, in particular, at temperatures above 200°C. The F-P conduction shows $\ln(I/E)$ linearly correlated with $E^{1/2}$ (Fig. 3d), and the current can be expressed by Eq. 3.[7] As for the comb capacitors with an α-SiCN/α-SiC bilayer barrier of 40 nm/10 nm or 30 nm/20 nm thickness, F-P conduction prevails at electric fields above 0.5 MV/cm

$$\text{ohmic} \quad I \sim E \exp(-c/T) \qquad [1]$$

$$\text{SE} \quad I \sim T^2 \exp(aE^{1/2}/T - q\Phi_B/kT) \qquad [2]$$

$$\text{F-P} \quad I \sim E \exp(2aE^{1/2}/T - q\Phi_B/kT) \qquad [3]$$

where c is a constant, a represents $(q/4\pi\varepsilon d)^{1/2}$, ε is the dielectrics dynamic permittivity, d is the dielectrics thickness, and Φ_B is the barrier height of electrons into the conduction band. Table I summarizes the leakage mechanisms at various electric fields for the Cu comb capacitors measured at temperatures of 200-250°C. The leakage mechanism between the Cu lines is dependent on the thickness ratio of the α-SiCN/α-SiC bilayer barrier. In contrast to the α-SiCN (50 nm)/α-SiC (2 nm) sample, there is a transition of SE to F-P conduction at 0.8 MV/cm electric field in the α-SiCN (45 nm)/α-SiC (5 nm) sample, while the α-SiCN (40 nm)/α-SiC (10 nm) and α-SiCN (30 nm)/α-SiC (20 nm) samples exhibit the same leakage mechanisms at all electric fields employed in this study. Figure 4 shows the leakage current of various Cu comb capacitors *vs.* measurement temperature. Notably, the leakage current behavior at the low electric field of 0.65 MV/cm can be divided into two groups, with α-SiCN (50 nm)/α-SiC (2 nm) and α-SiCN (45 nm)/α-SiC (5 nm) samples in one group (Fig. 4a); at the high electric field of 1.25 MV/cm, however, the leakage current behavior of the α-SiCN (45 nm)/α-SiC (5 nm) sample shows that it deviates from that of the α-SiCN (50 nm)/α-SiC (2 nm) sample (Fig. 4b). This is due to the transition of SE to F-P conduction in the α-SiCN (45 nm)/α-SiC (5 nm) sample at 0.8 MV/cm electric field at elevated temperatures.

The leakage current density of the bulk OSG is at least 20 times larger than that of the bulk α-SiCN, α-SiC, α-SiCO (ESL), and PECVD oxide (ILD) films studied using MIS capacitors; thus, the effective leakage current component through the bulk OSG (250

[c] Raphael modeling is provided by Avant! business unit.

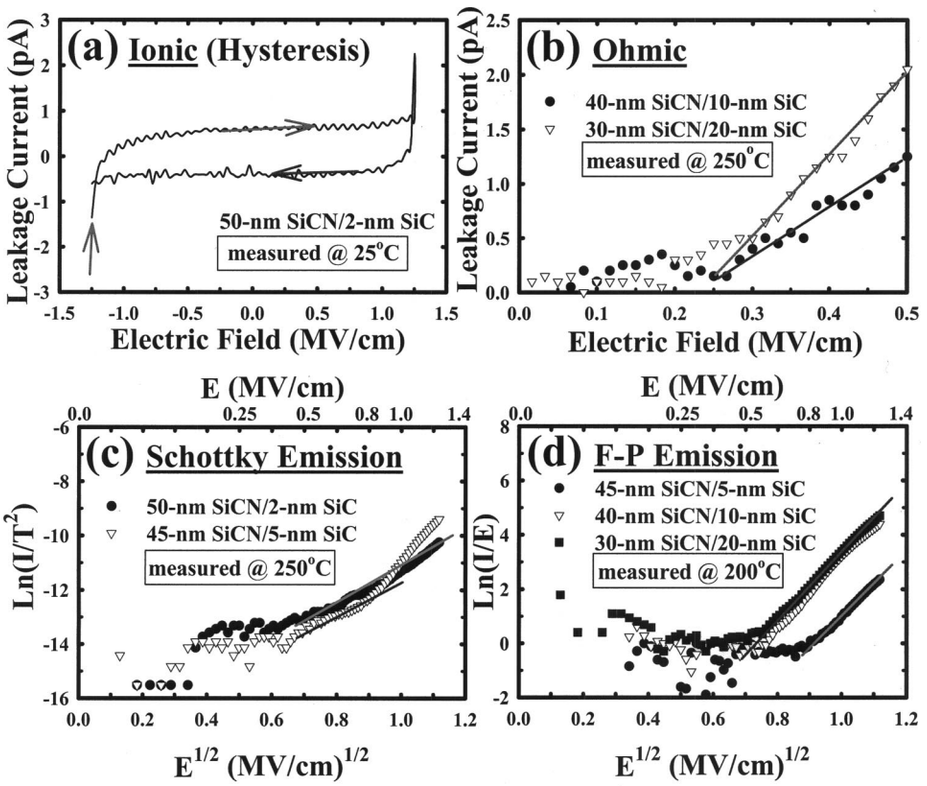

Figure 3. Conduction mechanism of (a) ionic, (b) ohmic, (c) Schottky emission, and (d) F-P emission for the Cu comb capacitor with a bilayer-structured Cu-cap barrier of various α-SiCN/α-SiC bilayer thicknesses.

nm) is expected to be at least two orders of magnitude larger than that through the α-SiCN (≤50 nm), α-SiC (≤20 nm), ESL (40 nm), and ILD (≤10 nm below ESL) dielectric films in the Cu comb capacitors. However, it has been reported that the localized surface defects at the α-SiC/OSG interface (CMP surface) can degrade the leakage current and TDDB reliability.[9,10] Because there is no CMP-induced damage at the OSG/ESL and ESL/ILD interfaces, we did not observe the pseudo-breakdown phenomenon, which supposedly arises from the defects at the OSG/ESL and ESL/ILD interfaces.[11] This is further discussed later and illustrated in Fig. 8. Therefore, the dominant leakage path in the Cu comb capacitor could be the electronic current through the bulk of OSG and/or the α-SiC/OSG interface. Possible determining factors for the dominant leakage path in the Cu comb capacitor may include the electric field and/or physical stress at the α-SiC/OSG interface and/or in the bulk of OSG. Figure 5 shows the electric field at the α-SiC/OSG interface and in the bulk of OSG obtained from Raphael simulation for various Cu comb capacitors biased with an electric voltage of 24 V. The higher electric field at the α-SiC/OSG interface than that in the bulk of OSG may be due to a number of factors, such as shorter distance at the top of Cu lines, angular shape at the corner of Cu lines, and higher dielectric constant of the α-SiC layer.[9] Because the behavior of the simulation-obtained electric field is contrary to the magnitude of leakage current with respect to the bilayer thickness ratio of the Cu comb capacitors, we presume that the increase leakage current between Cu lines for the α-SiCN (40 nm)/α-SiC (10 nm) and α-SiCN (30 nm)/α-SiC (20 nm) samples is attributed to the physical stress. Because the OSG film exhibits a tensile stress of 40-60 MPa, a compressive stress should be preferred for the α-SiC film deposited on top of the OSG layer.[2] However, the α-SiC film has a tensile stress of 10-20 MPa, and a thicker α-SiC film would be subjected to a larger tensile force,[12] which may generate a large number of interfacial defects, such as cracks, voids, traps or dangling bonds at the α-SiC/OSG interface, as illustrated in Fig. 6. For the Cu comb capacitors with α-SiCN (40 nm)/α-SiC (10 nm) and α-SiCN (30 nm)/α-SiC (20 nm) bilayer thicknesses, which exhibit a larger leakage current at temperatures above 200°C, the ohmic conduction dominates at an electric field between 0.25 and 0.5 MV/cm and the current is carried by thermally excited electrons hopping from one isolated trap to the next,[7] as shown in Table I. At an electric field above 0.5 MV/cm, the current is dominated by the F-P emission which is due to field-enhanced thermal excitation of trapped electrons into the conduction band.[7] Both the ohmic conduction and the F-P emission mechanisms result from a large number of interfacial defects at the α-SiC/OSG interface.

Figure 7 shows the breakdown field measured at 200°C for various comb capacitors with the data obtained from ten randomly chosen samples in each case. All samples exhibit a comparable breakdown field and the breakdown is presumably due to dielectric breakdown in the bulk of OSG rather than that at the α-SiC/OSG interface; the large variation of the breakdown field possibly results from the discordant force of manual probing and/or unfavorable samples at the wafer edge. Figure 8 shows the TDDB lifetime of various comb capacitors under different BTS conditions with the data obtained from six randomly chosen samples. It is found that all the comb capacitors reveal a comparable TDDB lifetime under a given BTS condition. The fact that the breakdown field (Fig. 7) and the TDDB lifetime (Fig. 8) of the Cu comb capacitors show little dependence on the thickness ratio of the α-SiCN/α-SiC bilayer bar-

Table I. Leakage mechanisms at various electric fields measured at 200-250°C for Cu comb capacitors with a bilayer-structured Cu-cap barrier of various α-SiCN/α-SiC bilayer thicknesses.

Electric field (MV/cm)	α-SiCN/α-SiC bilayer thickness (nm/nm)			
	50/2	45/5	40/10	30/20
0-0.25	Ionic	Ionic	Ionic	Ionic
0.25-0.5	Ionic	Ionic	Ohmic	Ohmic
0.5-0.8	SE	SE	F-P	F-P
0.8-1.25	SE	F-P	F-P	F-P

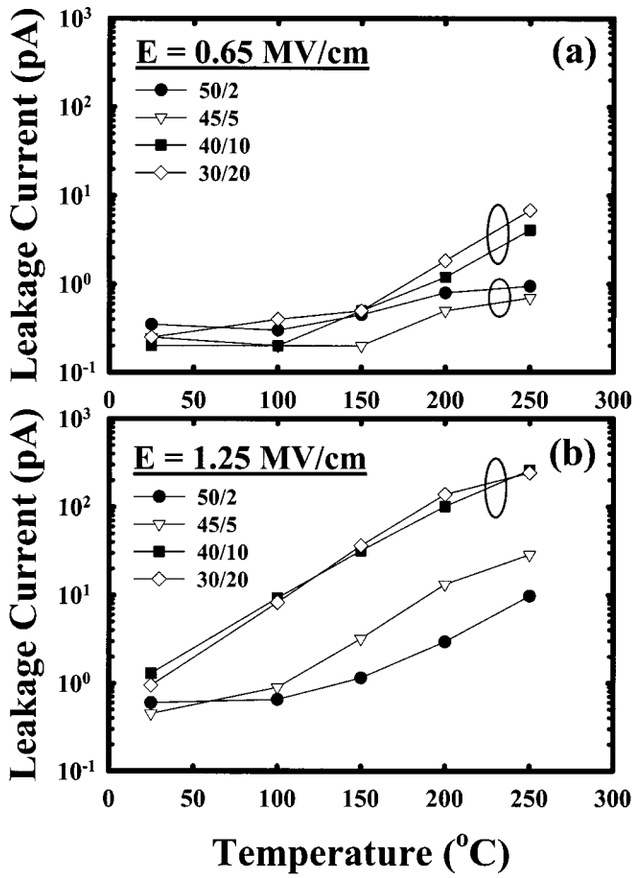

Figure 4. Leakage current as a function of temperature measured at an electric field of (a) 0.65 and (b) 1.25 MV/cm for the Cu comb capacitor with a bilayer-structured Cu-cap barrier of various α-SiCN/α-SiC bilayer thicknesses.

rier implies that the breakdown is very likely due to dielectric breakdown in the bulk of the OSG. Figure 9 illustrates the proposed leakage paths of the Cu comb capacitor studied in this work. We may conclude that the leakage and breakdown mechanisms in the

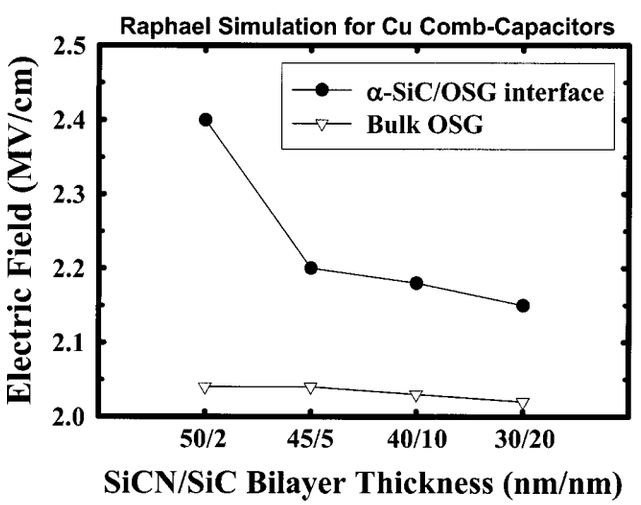

Figure 5. Electric field at the α-SiC/OSG interface and in the bulk of OSG obtained from Raphael simulation for various Cu comb capacitors biased with an electric voltage of 24 V.

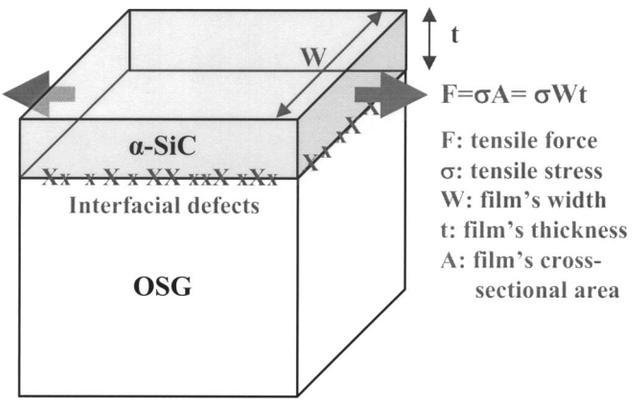

Figure 6. Schematic diagram showing the interfacial defects generated by the tensile force of the α-SiC film.

Cu comb capacitor with an α-SiCN/α-SiC bilayer barrier is closely correlated with the quality of the α-SiC/OSG interface and the OSG layer.

Conclusion

It is found that the leakage mechanism between Cu lines is dependent on the thickness ratio of the α-SiCN/α-SiC bilayer barrier in the Cu comb capacitor. Using an α-SiCN (40 nm)/α-SiC (10 nm)

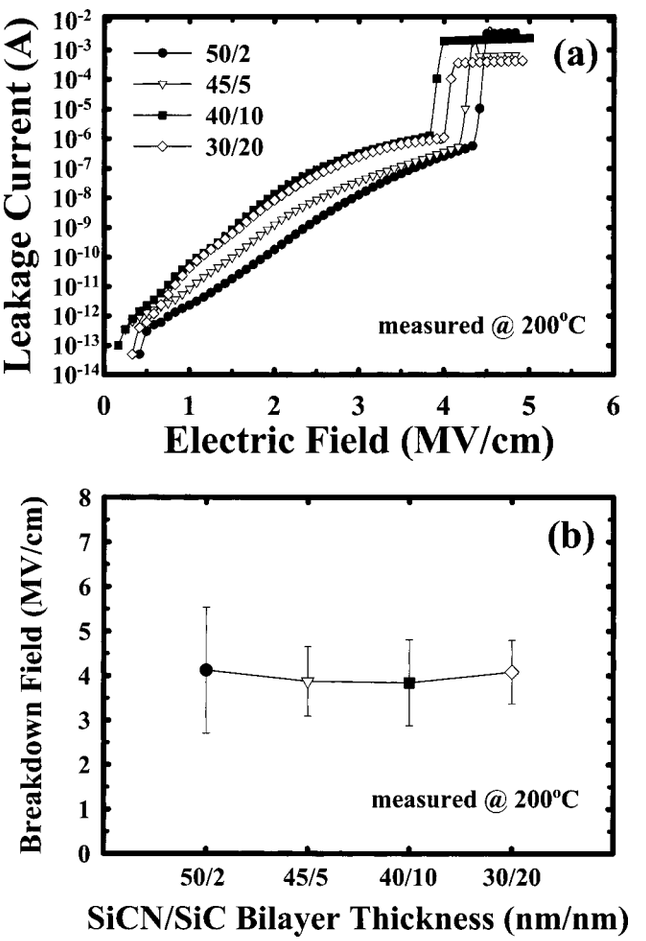

Figure 7. (a) Leakage current *vs.* electric field and (b) breakdown field for various Cu comb capacitors.

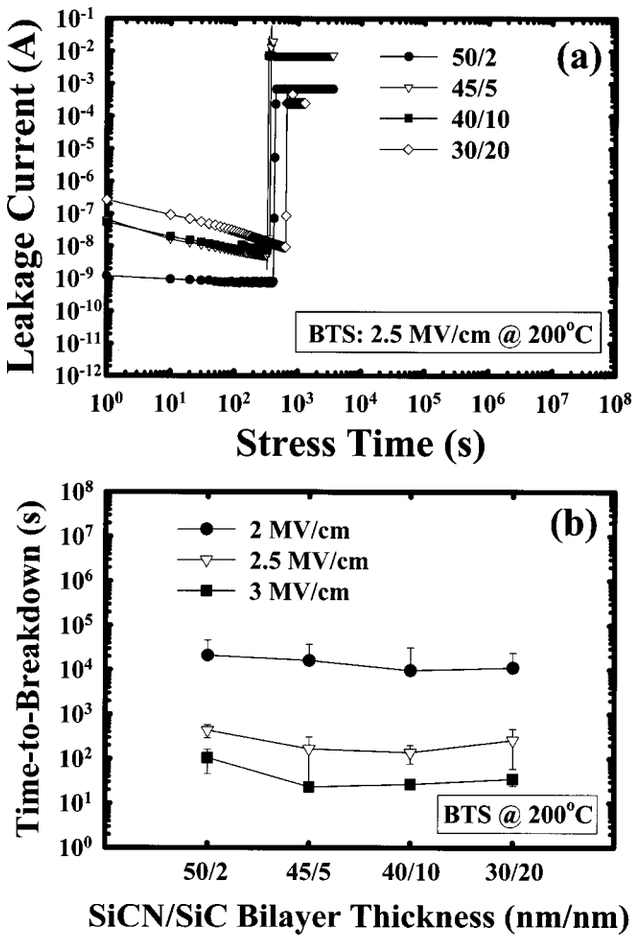

Figure 8. (a) TDDB under a BTS (2.5 MV/cm at 200°C) and (b) time-to-breakdown under different BTS conditions for various Cu comb capacitors.

or α-SiCN (30 nm)/α-SiC (20 nm) bilayer barrier, the increased leakage (F-P emission) between Cu lines is attributed to the large number of interfacial defects, such as cracks, voids, traps, or dangling bonds at the α-SiC/OSG interface, which are generated by the larger tensile force of the thicker α-SiC film. The Cu comb capacitor with an α-SiCN (50 nm)/α-SiC (2 nm) bilayer barrier exhibits a much smaller leakage current. The breakdown field and TDDB lifetime of the Cu comb capacitor reveal little dependence on the thickness ratio of the α-SiCN/α-SiC bilayer barrier, and the observed breakdown of the Cu comb capacitor is presumably due to dielectric breakdown of the bulk OSG layer.

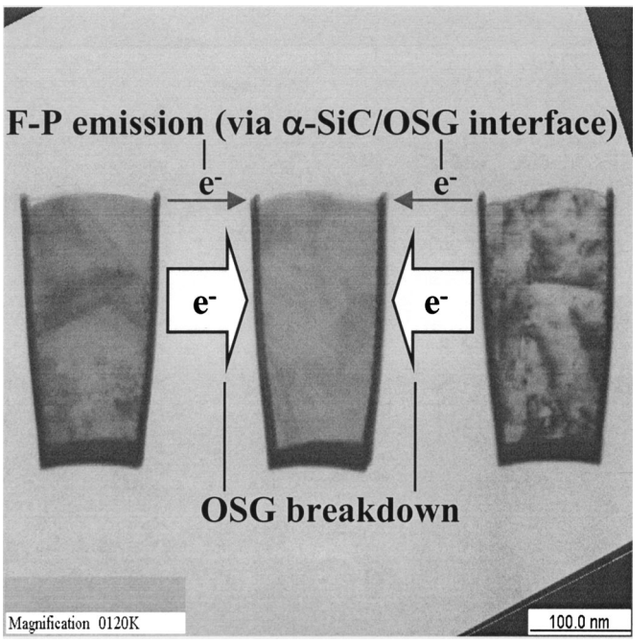

Figure 9. Proposed leakage paths of the Cu comb capacitor studied in this work.

Acknowledgment

The authors express their gratitude to Professor Bing-Yue Tsui of National Chiao-Tung University for his valuable discussion.

National Chiao-Tung University assisted in meeting the publication costs of this article.

References

1. J. Martin, S. Filipiak, T. Stephens, F. Huang, M. Aminpur, J. Mueller, E. Demircan, L. Zhao, J. Werking, C. Goldberg, S. Park, T. Sparks, and C. Esber, in *Proceedings of IEEE 2002 IITC*, p. 42 (2002).
2. M. Fayolle, J. Torres, G. Passemard, F. Fusalba, G. Fanget, D. Louis, L. Arnaud, V. Girault, J. Cluzel, H. Feldis, M. Rivoire, O. Louveau, T. Mourier, and L. Broussous, in *Proceedings of IEEE 2002 IITC*, p. 39 (2002).
3. F. Lanckmans, W. D. Gray, B. Brijs, and K. Maex, *Microelectron. Eng.*, **55**, 329 (2001).
4. K. L. Fang, B. Y. Tsui, C. C. Yang, and S. D. Lee, in *Proceedings of IEEE 2001 IITC*, p. 250 (2001).
5. P. Xu, K. Huang, A. Patel, S. Rathi, B. Tang, J. Ferguson, J. Huang, C. Ngai, and M. Loboda, in *Proceedings of IEEE 1999 IITC*, p. 109 (1999).
6. C. C. Chiang, M. C. Chen, Z. C. Wu, L. J. Li, S. M. Jang, C. H. Yu, and M. S. Liang, in *Proceedings of IEEE 2002 IITC*, p. 200 (2002).
7. S. M. Sze, *Physics of Semiconductor Devices*, 2nd ed., p. 402, John Wiley & Sons, New York (1981).
8. G. Bersuker, V. Blaschke, S. Choi, and D. Wick, in *Proceedings of IEEE 2000 IRPS*, p. 344 (2000).
9. J. Noguchi, T. Saito, N. Ohashi, H. Ashihara, H. Maruyama, M. Kubo, H. Yamaguchi, D. Ryuzaki, K. I. Takeda, and K. Hinode, in *Proceedings of IEEE 2001 IRPS*, p. 355 (2001).
10. S. U. Kim, T. Cho, and P. S. Ho, in *Proceedings of IEEE 1999 IRPS*, p. 277 (1999).
11. W. S. Song, T. J. Kim, D. H. Lee, T. K. Kim, C. S. Lee, J. W. Kim, S. Y. Kim, D. K. Jeong, K. C. Park, Y. J. Wee, B. S. Suh, S. M. Choi, H. K. Kang, K. P. Suh, and S. U. Kim, in *Proceedings of IEEE 2002 IRPS*, p. 305 (2002).
12. K. N. Tu, J. W. Mayer, and L. C. Feldman, *Electronic Thin Film Science*, p. 79, Macmillan Publishing, New York (1992).